DOI: 10.1021/ma101901y

Macromolecules
ARTICLE

Polymerization of Naturally Renewable Methylene Butyrolactones by Half-Sandwich Indenyl Rare Earth Metal Dialkyls with Exceptional Activity

Yangjian Hu,[†] Xin Xu,[‡] Yuetao Zhang,[†] Yaofeng Chen,*[,‡] and Eugene Y.-X. Chen*[,†]

[†]*Department of Chemistry, Colorado State University, Fort Collins, Colorado 80523-1872, United States , and* [‡]*State Key Laboratory of Organometallic Chemistry, Shanghai Institute of Organic Chemistry, Chinese Academy of Sciences, 354 Fenglin Road, Shanghai 200032, PRC*

Received August 18, 2010; Revised Manuscript Received September 25, 2010

ABSTRACT: Four discrete half-sandwich dialkyl rare earth metal (REM) complexes incorporating a disilylated indenyl ligand, (1,3-$(SiMe_3)_2C_9H_5$)M$(CH_2SiMe_3)_2$(THF) (M = Sc, Y, Dy, Lu), have been investigated for the coordination−addition polymerization of naturally renewable methylene butyrolactones, α-methylene-γ-butyrolactone (MBL) and γ-methyl-α-methylene-γ-butyrolactone (MMBL). Initial screening for the polymerization of methyl methacrylate highlighted several differences in catalytic behavior between these half-sandwich REM catalysts and well-studied sandwich REM catalysts in terms of reactivity trend, polymer tacticity, and solvent dependence. Most significantly, all four catalysts herein exhibit exceptional activity for polymerization of MMBL in DMF, achieving quantitative monomer conversion in <1 min with a 0.20 mol % catalyst loading and giving a high turnover frequency of $>30\,000\ h^{-1}$. Slower polymerizations occur in CH_2Cl_2, allowing for establishment of the activity trend within this REM series, which follows: Dy (largest ion) ≥ Y > Lu > Sc (smallest ion). The most active and effective Dy catalyst has been examined in detail, demonstrating its ability to control the polymerization for producing PMMBL with high T_g (221 °C) and with molecular weight ranging from a medium M_n of 1.89×10^4 Da to a high M_n of 1.63×10^5 Da, programmed by the [MMBL]/[Dy] ratio. Kinetic experiments have revealed a first-order dependence on [monomer] and a second-order dependence on [REM]. These kinetic results, coupled to catalyst efficiencies, NMR studies, as well as with chain-end group analysis by MALDI-TOF mass spectrometry, have yielded a chain initiation mechanism that involves both alkyl groups on each metal center and a bimolecular chain propagation that involves two metal centers in the rate-limiting C−C bond forming step. The Dy catalyst response to enolizable organo acids, externally added as chain-transfer agents, has also been examined.

Introduction

Typically employed in their neutral forms, rare earth metal (REM) catalysts for the coordination−addition polymerization of conjugate polar vinyl monomers offer two unique features over the more extensively investigated isoelectronic, cationic early transition-metal (group 4 in particular) catalysts: they require no cocatalysts and thus display no counteranion or ion-pairing effects on polymerization activity and stereochemistry.[1] The scope of polar vinyl monomers readily polymerizable by REM catalysts, especially bis(η^5-cyclopentadienyl) and related sandwich lanthanocene catalysts that often exhibit high polymerization activity and control,[2] has included methacrylates, in particular methyl methacrylate (MMA), acrylates, acrylamides, and acrylonitrile.[1] Compared with the prototypical sandwich REM catalysts, half-sandwich REM catalysts, despite their remarkable versatility demonstrated in the polymerization and copolymerization of olefins, especially styrene and isoprene, leading to a series of new polymeric materials,[3] have been studied to a much less extent for polymerization of polar vinyl monomers.[1] Notably, Yasuda and coworkers investigated the MMA polymerization by Cp*La$[CH(SiMe_3)_2]_2$(THF) in toluene at various temperatures and found that at −78 °C the resulting PMMA syndiotacticity was high (91% *rr*), but the activity, measured by turnover frequency (TOF = mol of substrate (monomer) consumed per mol catalyst (initiator) per h) and catalyst (or initiator) efficiency (I^* = M_n(calcd)/M_n(exptl)) were low, with TOF = 3 h^{-1} and I^* = ∼4%.[4] Upon increasing the reaction temperature to 0 and 25 °C, the activity drastically increased to 100 and 200 h^{-1} TOF, but the syndiotacticity dropped to 80 and 74% *rr*, respectively. Several other research groups have also reported the use of REM complexes incorporating half-sandwich-type ligands for polymerization of polar vinyl monomers, including linked Cp-amido ligands for acrylate and acrylonitrile polymerization by Okuda,[5] linked Cp-amino ligands for MMA polymerization by Cui,[6] linked fluorenyl-amido ligands for MMA polymerization by Carpentier,[7] boron-bridged indenyl-carboranyl ligands for MMA polymerization by Xie,[8] and nonlinked Cp-β-diketiminate ligands for MMA polymerization by Shen[9] and Schuchardt.[10] However, from polymerization control and syndiospecificity points of view, none of the above systems rivals the simple Cp*-based system reported by Yasuda.[4]

As petroleum resources continue to be depleted, there exists an imminent challenge of gradually replacing existing petroleum-based polymeric materials with those derived from naturally occurring, renewable resources in a technologically and economically competitive fashion.[11] In this context, naturally renewable methylene butyrolactone monomers, such as α-methylene-γ-butyrolactone (MBL) and γ-methyl-α-methylene-γ-butyrolactone (MMBL), are of particular interest in exploring the prospects of

*Corresponding authors. E-mail: yaofchen@mail.sioc.ac.cn (Y.C.); eugene.chen@colostate.edu (E.C.).

 Published on Web 10/22/2010

Scheme 1. Renewable Methylene Butyrolactone Monomers (M)MBL and Polymers P(M)MBL versus MMA and PMMA As Well As Structures of Half-Sandwich REM Dialkyl Catalysts

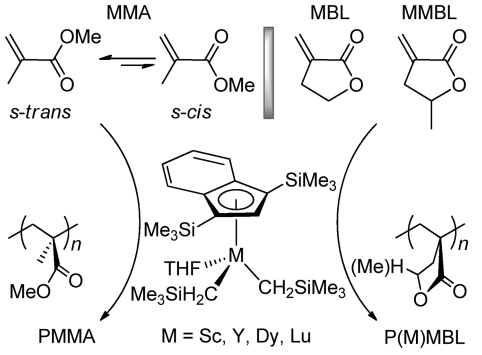

substituting the petroleum-based methacrylate monomers for specialty chemicals production.[12] MBL, or tulipalin A, is a natural substance found in tulips, and the MBL ring is an integral building block of many (~10% known) natural products,[13] whereas its γ-methyl derivative, MMBL, is readily prepared via a two-step process from the cellulosic biomass-derived levulinic acid.[14] As the cyclic analog of MMA, MBL exhibits greater reactivity in free radical polymerization[15] than MMA, attributable to the presence of both the nearly planar five-membered lactone ring (which provides a high degree of resonance stabilization for the active radical species) and the higher energy exocyclic C=C double bond (as a result of the ring strain and the fixed s-cis conformation)[16] (Scheme 1). The cyclic ring in MBL also imparts significant enhancements in the materials properties of the resulting PMBL due to the conformational rigidity of the polymer chain through incorporation of the butyrolactone moiety. For example, the glass-transition temperature (T_g) of PMBL produced by the radical polymerization is 195 °C,[17] which is ~90 °C higher than that of atactic PMMA. Additionally, compared with PMMA, PMBL exhibits increased optical properties as well as resistance to solvent, heat, and scratch.[18]

Polymerization of MBL has been investigated predominately using various free-radical polymerization mechanisms,[15−17,19] but several other types of mechanisms, including group-transfer polymerization,[20] anionic polymerization,[17] and coordination polymerization by metallocene complexes,[21] have also been explored. MBL has been copolymerized with various comonomers[15] such as MMA,[22] styrene,[19c,23] methoxystyrene,[24] and vinyl thiophenes.[25] In comparison, the polymerization of MMBL has been studied to a much lesser extent. Nevertheless, MMBL has also been free radically copolymerized with styrene and MMA,[26] polymerized by free-radical emulsion polymerization[27,28] as well as polymerized by free-radical, anionic, and group-transfer polymerization methods, which required long reaction times (2 to 44 h), often at low temperatures, achieving low to high but never complete conversions with unknown polymerization and polymer molecular weight (MW) characteristics.[29] Most recently, we found that the coordination polymerization of MBL and MMBL in DMF by the divalent $Cp^*_2Sm(THF)_2$ catalyst is fast (TOF $\approx$ 3000 h^{-1}), efficient (I^* approaching 100%), and controlled, leading to PMBL and PMMBL with relatively narrow MW distributions (MWDs) as well as their diblock copolymers with MMA or with each other.[21] We also recently reported the high-speed and living polymerization of MBL and MMBL by a bifunctional silicon catalyst system consisting of both the nucleophilic silyl ketene acetal initiating moiety and the electrophilic silylium R_3Si^+ catalyst.[30] Atactic PMMBL produced exhibits a T_g of 225 °C, representing a T_g enhancement of ~120 °C over the T_g of the typical atactic PMMA.

In light of the above overviewed remarkable activity and control demonstrated by metal and metalloid catalysts for the polymerization of renewable (M)MBL, especially by sandwich lanthanocene catalysts, we were intrigued by the prospects of half-sandwich REM catalysts for (M)MBL polymerization for two reasons: (a) they have not been examined for this type of polymerization and (b) they have shown some unique catalytic behavior in polymerization of other monomers, particularly olefins and MMA (vide supra). Accordingly, the central objective of this study was to examine the characteristics of (M)MBL polymerizations using the following discrete half-sandwich REM dialkyl catalysts incorporating the disilylated indenyl ligand (Scheme 1): $(1,3\text{-}(SiMe_3)_2C_9H_5)M(CH_2SiMe_3)_2(THF)$ (M = Sc,[31] Y,[32] Dy,[32] Lu[32]).

Experimental Section

Materials and Methods. All syntheses and manipulations of air- and moisture-sensitive materials were carried out in flamed Schlenk-type glassware on a dual-manifold Schlenk line, a high-vacuum line, or in an argon or nitrogen-filled glovebox. HPLC-grade organic solvents were sparged extensively with nitrogen during filling of the solvent reservoir and then dried by passage through activated alumina (for Et_2O, THF, and CH_2Cl_2), followed by passage through Q-5-supported copper catalyst (for toluene and hexanes) stainless steel columns. HPLC-grade DMF was degassed and dried over CaH_2 overnight, followed by vacuum transfer (no distillation). NMR solvents $CDCl_3$ and DMSO-d_6 were dried over activated Davison 4 Å molecular sieves, and NMR spectra were recorded on a Varian Inova 300 (FT 300 MHz, ^1H; 75 MHz, ^{13}C), a Varian Inova 400 MHz, or an Inova 500 MHz spectrometer. Chemical shifts for ^1H and ^{13}C spectra were referenced to internal solvent resonances and are reported as parts per million relative to tetramethylsilane.

Monomers MBL and MMBL were purchased from TCI America, whereas MMA, 3-methyl-2-butanone (MBO), and methyl isobutyrate (MIB) were purchased from Aldrich. These chemicals were degassed and dried over CaH_2 overnight, followed by vacuum distillation, while MMA was further purified by titration with neat tri(*n*-octyl)aluminum (Strem Chemical) to a yellow end point,[33] followed by vacuum distillation. Butylated hydroxytoluene (BHT-H, 2,6-di-*tert*-butyl-4-methylphenol) was purchased from Aldrich and was recrystallized from hexanes prior to use. Activator $[Ph_3C][B(C_6F_5)_4]$ (TPB)[34] was obtained as a research gift from Boulder Scientific and used as received. Literature procedures were employed to prepare the following compounds: $(1,3\text{-}(SiMe_3)_2C_9H_5)M(CH_2SiMe_3)_2(THF)$ (M = Sc,[31] Y,[32] Dy,[32] Lu[32]), $[(1,3\text{-}(SiMe_3)_2C_9H_5)Sc(CH_2SiMe_3)(THF)_x]^+[B(C_6F_5)_4]^-$,[31] and trityl[tris(tetrachlorobenzenediolato) phosphate(V)] $[Ph_3C][rac\text{-}TRISPHAT]$ (TTP).[35]

General Polymerization Procedures. Polymerizations were performed either in 25 mL flame-dried Schlenk flasks interfaced to the dual-manifold Schlenk line for runs using external temperature bath or in 30 mL glass reactors inside the glovebox for ambient temperature (ca. 25 °C) runs. In a typical polymerization procedure, a predetermined amount of REM catalyst (11.7 μmol for runs with a [MMA]/[catalyst] ratio of 400 or 10.2 μmol for runs with a [MMBL]/[catalyst] ratio of 400) was dissolved in a solvent (4.5 mL of toluene or 3.0 mL of DCM, DMF and THF). With vigorous stirring, monomer (MMA, 0.50 mL, 4.68 mmol; MBL, 0.33 mL, 3.77 mmol; or MMBL, 0.44 mL, 4.08 mmol) was quickly added to the above catalyst solution via syringe to start the polymerization. For polymerizations by the in situ generated cationic Sc catalyst, the neutral Sc complex and the trityl activator, TPB or TTP, was premixed in toluene for 10 min before addition of monomer. For polymerizations with an added chain-transfer agent (CTA), the monomer and CTA were premixed before the mixture was added to the catalyst solution. For (M)MBL polymerizations in DMF, THF, and DCM, toluene (289 μL, 2.72 mmol) was added as an

Table 1. Selected Results of MMA Polymerization by REM (Sc, Y, Dy, Lu) Dialkyls (0.25 mol %)[a]

run no.	REM cat.	solvent	conv. (%)[b]	$10^4 M_n$ (g/mol)[c]	MWD (M_w/M_n)[c]	I^* (%)[d]	[*rr*] (%)[b]	[*mr*] (%)[b]	[*mm*] (%)[b]
1	Sc	TOL	42.5	2.35	1.44	73	81.0	18.5	0.5
2	Y	TOL	12.4	1.97	1.49	26	40.9	25.0	34.1
3	Dy	TOL	< 1	n.d.	n.d.	n.d.	n.d.	n.d.	n.d.
4	Lu	TOL	8.6	n.d.	n.d.	n.d.	46.5	23.5	30.0
5	Sc	DCM	49.6	2.05	1.37	97	82.4	15.7	1.9
6	Sc	THF	0						
7	Sc	DMF	78.8	4.61	1.69	69	67.3	32.5	0.2
8	Y	DMF	80.1	6.87	2.09	47	61.2	34.6	4.2
9	Dy	DMF	84.0	8.64	2.14	38	58.4	38.1	3.5
10	Sc/TPB	TOL	28.2	2.87	1.47	40	74.1	22.7	3.2
11	Sc/TTP	TOL	17.1	2.44	1.68	28	66.6	19.9	13.5

[a] Conditions: 4.5 mL (TOL: toluene, DCM: CH_2Cl_2) or 3.0 mL (DMF: dimethylformamide, THF: tetrahydrofuran) of solvent, 0.50 mL of MMA (4.68 mmol); 11.7 μmol REM complex (except for runs 10 and 11, where equimolar activator TPB: $[Ph_3C]^+[B(C_6F_5)_4]^-$ or TTP: $[Ph_3C]^+$-[*rac*-TRISPHAT]$^-$ was added); [MMA]/[REM] 400/1; ~25 °C; 24 h; n.d. = not determined. [b] Monomer conversions and polymer methyl triads measured by ^{1}H NMR. [c] Determined by GPC relative to PMMA standards. [d] Initiator efficiency (I^*) = M_n(calcd)/M_n(exptl), where M_n(calcd) = MW(monomer) × [monomer]/[catalyst] × conversion% + MW of chain-end groups (88.2), assuming one chain initiation per metal center.

internal standard to the reaction mixture. After the measured time interval, a 0.2 mL aliquot was taken from the reaction mixture via syringe and quickly quenched into a 4 mL vial containing 0.6 mL of undried "wet" $CDCl_3$ stabilized by 250 ppm of BHT-H; the quenched aliquots were later analyzed by ^{1}H NMR to obtain the percent monomer conversion data. The polymerization was immediately quenched after the removal of the aliquot by the addition of 5 mL of 5% HCl-acidified methanol. The quenched mixture was precipitated in 100 mL of methanol, stirred for 1 h, filtered, washed with methanol, and dried in a vacuum oven at 50 °C overnight to a constant weight.

The ratio of $[MMA]_0/[MMA]_t$ at a given time t was determined by integration of the peaks for MMA (5.2 and 6.1 ppm for the vinyl signals; 3.4 ppm for the OMe signal) and PMMA (centered at 3.4 ppm for the OMe signals) according to $[MMA]_0/[MMA]_t = 2\mathbf{A}_{3.4}/3\mathbf{A}_{5.2+6.1}$, where $\mathbf{A}_{3.4}$ is the total integrals for the peaks centered at 3.4 ppm (typically in the region 3.2 to 3.6 ppm) and $\mathbf{A}_{5.2+6.1}$ is the total integrals for both peaks at 5.2 and 6.1 ppm. For (M)MBL polymerizations, we calculated monomer percent conversions by comparing the integration of the vinyl protons of the unreacted monomer with the methyl protons of toluene added as internal standard.

^{1}H NMR ($CDCl_3$, 300 MHz, 23 °C) for PMMA: δ 3.60 (s, O*Me*), 2.05 (d, CH_2), 1.99−1.90 (m, CH_2), 1.82 (s, CH_2), 1.48 (d, CH_2), 1.22 (s, CH_3, *mm*), 1.02 (s, CH_3, *mr*), 0.85 (s, CH_3, *rr*). ^{1}H NMR (DMSO-d_6, 300 MHz, 100 °C) for PMBL: δ 4.34 (b.s, 2H, OCH_2), 2.24−1.99 (m, 4H, CH_2, CH_2). ^{13}C NMR (DMSO-d_6, 125 MHz, 100 °C) for PMBL: δ 179 (*C*═O), 64.36 (O*C*H$_2$), 44.22, 43.90, 43.74 (quaternary carbon, *rr*, *mr*, *mm*), 41.89−40.58 (main-chain *C*H$_2$, unresolved tetrads), 30.47 (β-*C*H$_2$). ^{1}H NMR (DMSO-d_6, 300 MHz, 100 °C) for PMMBL: δ 4.64 (b.s, 1H, C*H*), 2.31 (b.s, 2H, CH_2), 1.99 (b.s, 2H, CH_2), 1.39 (b.s, 3H, CH_3). ^{13}C NMR (DMSO-d_6, 125 MHz, 100 °C) for PMMBL: δ 178 (*C*═O), 72.65 (O*C*H), 46.48, 46.15, 45.80 (quaternary carbon, *rr*, *mr*, *mm*), 43.05 (β-*C*H$_2$), 40.53, 39.19, 37.69 (main-chain *C*H$_2$, *rr*, *mr*, *mm*), 19.46 (*C*H$_3$). DEPT experiments were used to remove the DMSO signals in the ^{13}C NMR experiments.

Polymerization Kinetics. Kinetic experiments were carried out in a stirred glass reactor at ambient temperature (ca. 25 °C) inside an argon-filled glovebox using the procedure already described above and with $[MMBL]_0/[Dy]_0$ ratios of 200:1, 400:1, 800:1, 1200:1, and 1600:1, where $[MMBL]_0$ = 1.09 M and $[Dy]_0$ = 5.47, 2.74, 1.37, 0.912, and 0.684 mM in 3.73 mL of CH_2Cl_2 + MMBL + toluene (internal standard) solutions. At appropriate time intervals, 0.2 mL aliquots were withdrawn from the reaction mixture using syringe and quickly quenched in 1 mL septum-sealed vials containing 0.6 mL of undried "wet" $CDCl_3$ mixed with 250 ppm BHT-H. The quenched aliquots were analyzed by ^{1}H NMR to obtain monomer conversions. Apparent rate constants (k_{app}) were extracted by linearly fitting a line to the plot of $\ln([MMBL]_0/[MMBL]_t)$ versus time.

Polymer Characterizations. The low-molecular-weight PMMBL sample was analyzed by matrix-assisted laser desorption/ionization time-of-flight mass spectroscopy (MALDI−TOF MS); the experiment was performed on an Ultraflex MALDI-TOF mass spectrometer (Bruker Daltonics) operated in positive ion reflector mode using a Nd/YAG laser at 355 nm and 25 kV accelerating voltage. A thin layer of a 1% NaI solution was first deposited on the target plate, followed by 1 μL of both sample and matrix (2,5-dihydroxy benzoic acid, 10 mg/mL in 50% CAN, 0.1% TFA). External calibration was done using a peptide calibration mixture (four to six peptides) on a spot adjacent to the sample. The raw data were processed in the FlexAnalysis software (version 2.4, Bruker Daltonics).

Polymer number-average molecular weights (M_n) and molecular weight distributions (MWD = M_w/M_n) were measured by gel permeation chromatography (GPC) analyses carried out at 40 °C and a flow rate of 1.0 mL/min, with $CHCl_3$ as the eluent for PMMA or with DMF for PMBL and PMMBL, on a Waters University 1500 GPC instrument coupled to a Waters RI detector and equipped with four PLgel 5 μm mixed-C columns (Polymer Laboratories; linear range of MW = 200−2 000 000). The instrument was calibrated with 10 PMMA standards, and chromatograms were processed with Waters Empower software (version 2002). Glass-transition temperatures (T_g) of the polymers were measured by differential scanning calorimetry (DSC) on a DSC 2920, TA Instrument. Polymer samples were first heated to 150 at 20 °C/min, equilibrated at this temperature for 4 min, then cooled to 30 at 20 °C/min, held at this temperature for 4 min, and reheated to 300 at 10 °C/min. All T_g values were obtained from the second scan after the thermal history was removed. ^{1}H NMR spectra for the analysis of PMMA microstructures were recorded in $CDCl_3$ at 50 °C and analyzed according to the literature methods,[36] whereas tacticities of PMBL[15,20] and PMMBL[29] were measured by ^{13}C NMR in DMSO-d_6 at 100 °C.

Results and Discussion

Characteristics of MMA Polymerization. We first screened the activity of the four half-sandwich REM dialkyl catalysts toward MMA polymerization at RT with a fixed catalyst loading of 0.25 mol % and reaction time of 24 h in different solvents (toluene, DCM, THF, and DMF), the results of which were summarized in Table 1. Three polymerization features are noteworthy when compared with those of the prototype sandwich lanthanocene catalyst Cp*$_2$LnMe(THF) or [Cp*$_2$SmH]$_2$. First, in relatively nonpolar toluene (ε = 2.38), the smallest Sc catalyst achieved the highest monomer conversion of 42.5%, producing PMMA with an appreciable syndiotacticity of 81.0% *rr* (run 1), whereas other REM catalysts exhibited either only marginal (Dy, run 3) or low (Y, run 2; Lu, run 4) activity. This observation

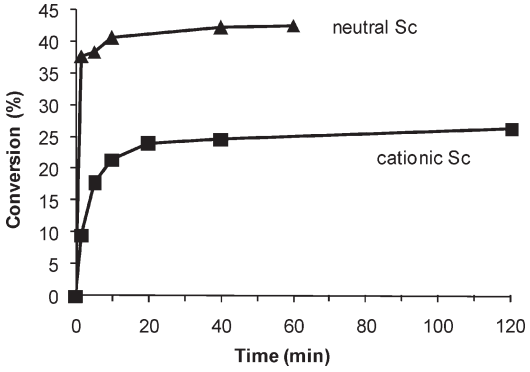

Figure 1. Conversion versus time plots of MMA polymerization in toluene at RT by the neutral Sc catalyst (▲, run 1) and by the cationic Sc catalyst (■, run 10).

was unexpected because the MMA polymerization activity of prototype lanthanocene catalysts $Cp^*_2LnMe(THF)$ typically increases with an increase in ionic radii of the Ln metal.[37] Second, moving to more polar (ε = 8.93), noncoordinating DCM noticeably enhanced the MMA conversion (to 49.6%), catalyst efficiency (I^* = 97%), and the PMMA syndiotacticity (82.4% *rr*), run 5. This level of syndiotacticity for the PMMA produced at RT is noteworthy because it is higher than the syndiotacticity of the PMMA produced by arguably the best lanthanocene catalyst, $[Cp^*_2SmH]_2$ or $Cp^*_2SmMe(THF)$, at 25 °C and equals that produced at 0 °C.[37] Third, unlike lanthanocene catalysts such as $Cp^*_2SmMe(THF)$, which can tolerate polar, coordinating solvents such as THF (ε = 7.58) without noticeably altering the polymerization results,[37] the half-sandwich Sc catalyst was completely inactive for MMA polymerization in THF (run 6) but exhibited good activity in more polar DMF (ε = 36.7), achieving 78.8% conversion, at the expense of lowered syndiotacticity (67.3% *rr*). Intriguingly, while being only marginally active in toluene, the Dy catalyst achieved the highest conversion (84%, run 9) in DMF within this catalyst series. All PMMA produced by these half-sandwich REM catalysts, under various conditions, showed unimodal MWDs with M_w/M_n values ranging from 1.37 to 2.14, typical for single-site catalysts.

Prompted by the unique catalytic behavior of the cationic half-sandwich REM catalysts observed for olefin polymerization,[3] we also examined the MMA polymerization by the cationic half-sandwich Sc complex[31] derived from in situ activation of the corresponding neutral Sc complex with the activator $[Ph_3C]^+[B(C_6F_5)_4]^-$. Compared with the neutral catalyst, the cationic catalyst achieved 14% lower monomer conversion (run 10 vs run 1) and also produced PMMA with 7% lower syndiotacticity (run 10 vs run 1). The cation derived from activation with another trityl activator, $[Ph_3C]^+$-[*rac*-TRISPHAT]$^-$, was even worse in all polymerization characteristics (run 11). However, monitoring of the MMA polymerizations by the neutral and cationic Sc catalysts revealed that both systems incurred nearly total catalyst deactivation after achieving their respective near maximum conversions (~43% for the neutral catalyst and ~25% for the cationic catalyst) over a short reaction time period (~10 and ~20 min, respectively, Figure 1), upon which time there was no significant further increase in monomer conversion, even up to 24 h.

Overall, except for the impressive PMMA syndiotacticity achieved by the Sc catalyst in DCM at RT, these half-sandwich REM complexes are relatively poor catalysts for MMA polymerization, as evidenced by their inability to achieve high monomer conversions because of substantial catalyst deactivation under the current conditions (RT, 0.25 mol % catalyst loading). On the other hand, the current REM catalysts are highly active for polymerization of MMBL, achieving quantitative monomer conversion in 1 min (vide infra), which presumably reflects the relative stability of the propagating REM enolate species toward β-alkoxide elimination, the most common type of termination involved in group 4 catalysts.[1,38]

Table 2. Results of MBL Polymerization by REM (Sc, Y, Dy, Lu) Dialkyls[a]

run no.	REM cat.	conv. (%)	10^3M_n (g/mol)	MWD (M_w/M_n)	I^* (%)
12	Sc	38.4	8.40	1.87	167
13	Y	87.7	9.60	1.67	333
14	Dy	88.1	15.4	1.84	208
15	Lu	39.9	12.5	1.78	116

[a] Conditions: 3.0 mL of DMF, 3.77 mmol MBL, 10.2 μmol REM complex, [MBL]/[REM] 370/1, ~25 °C, 24 h. See the footnotes under Table 1 for other explanations.

Characteristics of MBL and MMBL Polymerizations. Next, we investigated MBL polymerization by these four half-sandwich REM catalysts. Owing to insolubility of the resulting PMBL in common organic solvents other than DMF, the polymerizations were carried out in DMF, the results of which were summarized in Table 2. It can be seen from the Table that the polymerization (0.27 mol % catalyst loading, RT) was sluggish for the Sc and Lu catalysts, achieving only 38.4 (run 12) and 39.9% (run 15) monomer conversion after 24 h, respectively. Y and Dy catalysts achieved relatively high conversions of 87.7 (run 13) and 88.1% (run 14), respectively. Qualitatively, the activity trend seems to follow the ionic radii of these metals: the larger Dy and Y metals exhibited considerably higher activity than those smaller Lu and Sc metals. A unique feature demonstrated by these half-sandwich REM dialkyl catalysts in the polymerization of MBL was the observed much-greater-than 100% catalyst efficiency (from 116 to 333%), indicating that both alkyl groups on the metal participated in chain initiation or there existed internal chain transfer; further discussion will follow in the next section.

Excitingly, all four REM catalysts are exceptionally active for polymerization of MMBL in DMF at RT. With a catalyst loading of 0.25 mol %, all catalysts achieved near quantitative monomer conversion in 1 min, thus giving a high TOF of 24 000 h^{-1} (runs 16−19, Table 3). In fact, the polymerization by Dy with a lower catalyst loading of 0.20 mol % still requires < 1 min to achieve a quantitative monomer conversion, giving a TOF at least > 30 000 h^{-1} for this catalyst system, which is 10 times higher than the sandwich samarocene catalyst $Cp^*_2Sm(THF)_2$.[21] This drastic effect of γ-methyl substitution to the MBL ring on monomer activity is remarkable; because MBL is generally regarded as being more reactive than MMBL (larger monomer), the drastically higher activity of the MMBL polymerization than that of the MBL polymerization seen here must contribute to electronic effects (i.e., being more electron-rich, MMBL binds to REM more strongly) and substrate-catalyst structural matching (i.e., these sterically more accessible half-sandwich catalysts can more easily accommodate larger monomers). The MWD of the resulting PMMBL is respectable (≤1.87). Improved solubility of PMMBL in other common organic solvents, due to the methyl substitution, allowed us to investigate this polymerization in DCM and THF. The polymerization in DCM was slower, but all catalysts achieved a 100% monomer conversion in 20 min (Y, run 21; Dy, run 22), 30 min (Lu, run 23), or 120 min (Sc, run 20). These results reaffirmed the activity trend seen in the MBL polymerization (i.e., Dy ≥ Y > Lu > Sc): the largest Dy and Y metals are also most active for MMBL polymerization, whereas the smallest Sc

Table 3. Selected Results of MMBL Polymerization by REM (Sc, Y, Dy, Lu) Dialkyls[a]

run no.	REM cat.	solvent	time (min)	conv. (%)	$10^4 M_n$ (g/mol)	MWD (M_w/M_n)	I^* (%)	T_g (°C)
16	Sc	DMF	1	98.2	5.33	1.87	84	n.d.
17	Y	DMF	1	100	3.22	1.56	139	n.d.
18	Dy	DMF	1	100	3.69	1.64	122	n.d.
19	Lu	DMF	1	100	3.47	1.84	129	n.d.
20	Sc	DCM	120	100	3.55	1.99	127	217
21	Y	DCM	20	100	2.77	2.36	162	218
22	Dy	DCM	20	100	3.16	2.62	143	221
23	Lu	DCM	30	100	2.72	2.73	165	222

[a] Conditions: 3.0 mL of solvent, 4.08 mmol MMBL, 10.2 μmol REM complex, [MMA]/[REM] 400/1, toluene (0.29 mL, 2.72 mmol) added as internal standard, ~25 °C. See the footnotes under Table 1 for other explanations.

Table 4. Results of MMBL Polymerization by REM Dialkyls at Different [MMBL]/[REM] Ratios[a]

run no.	REM cat.	solvent	[MMBL]/[REM]	time (min)	conv. (%)	$10^4 M_n$ (g/mol)	MWD (M_w/M_n)	I^* (%)
24	Sc	THF	200	30	100	2.69	1.62	84
25	Sc	THF	400	360	100	4.58	2.07	98
26	Sc	THF	600	1200	100	5.61	2.02	120
27	Sc	THF	800	1440	83.3	7.22	1.89	104
28	Dy	DCM	200	1	100	1.89	1.99	119
29	Dy	DCM	400	20	100	3.16	2.62	143
30	Dy	DCM	800	40	100	6.80	2.27	132
31	Dy	DCM	1200	150	100	10.7	1.91	126
32	Dy	DCM	1600	240	100	16.3	1.65	110

[a] Conditions: 3.0 mL of solvent, 4.08 mmol MMBL with varied amounts of REM specified by the [MMBL]/[REM] ratio, 0.289 mL of toluene as internal standard, ~25 °C. See the footnotes under Table 1 for other explanations.

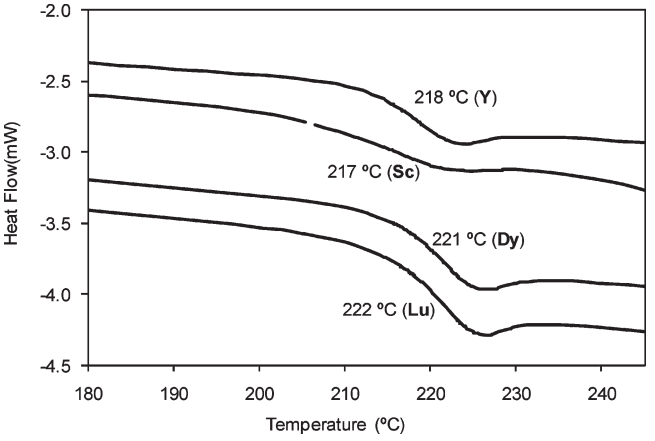

Figure 2. DSC plots of PMMBL (**Y**, $M_n = 2.77 \times 10^4$, run 21, Table 3; **Sc**, $M_n = 3.55 \times 10^4$, run 20, Table 3; **Dy**, $M_n = 3.16 \times 10^4$, run 22, Table 3; and **Lu**, $M_n = 2.72 \times 10^4$, run 23, Table 3).

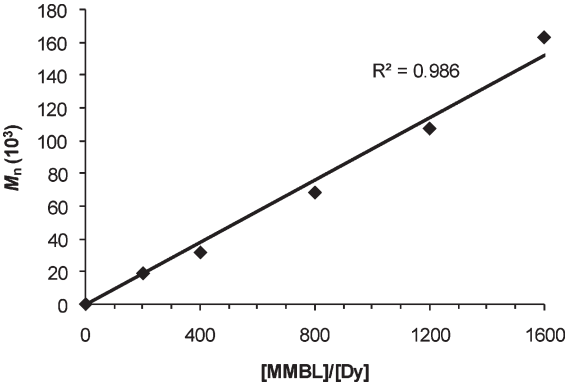

Figure 3. Plot of M_n of PMMBL versus the [MMBL]/[Dy] ratio for the polymerization of MMBL by the Dy catalyst in DCM at 25 °C, achieving a 100% monomer conversion for all runs (runs 28−32, Table 4).

catalyst is the least active, with the Lu catalyst lying somewhere in the middle. The T_g values of the syndio-rich atactic PMMBL (42.4% *rr*, 44.8% *mr*, 12.8% *mm*, run 22) produced herein are in the range of 217 to 222 °C (Figure 2), which are expected for typical atactic PMMBL.[30] Also consistent with the observation made in the MBL polymerization, the MMBL polymerization gave generally >100% catalyst efficiency (up to 165%).

In contrast with the inactivity of the Sc catalyst for MMA polymerization in THF, the polymerization of MMBL in THF by this catalyst is rapid (Table 4), effecting a quantitative monomer conversion in 30 min (0.5 mol % catalyst, run 24), 6 h (0.25 mol % catalyst, run 25), or 20 h (0.167 mol % catalyst, run 26). We also examined the degree of control over polymer MW by varying the [MMBL]/[Dy] ratio from 200 (0.5 mol % catalyst) to 1600 (0.0625 mol % catalyst). The polymerizations in DCM at all ratios achieved a 100% monomer conversion in short times, ranging from 1 min to 4 h, depending on the catalyst loading (runs 28−32). A plot of M_n of PMMBL versus the [MMBL]/[Dy] ratio gave a straight line ($R^2 = 0.986$, Figure 3), demonstrating a high degree of control over M_n by adjusting the monomer-to-catalyst ratio. Hence, PMMBL with a medium M_n of 1.89×10^4 and MWD of 1.99 (run 28) to a high M_n of 1.63×10^5 and MWD of 1.65 (run 32) can be readily prepared. Attempts to prepare stereoregular PMMBL by lowering the polymerization temperature were unsuccessful because the resulting polymer tacticity was not significantly affected by the polymerization temperature (from 25 °C, run 33, to −65 °C, run 35, Table 5).

Kinetics and Mechanism of MMBL Polymerization. Having established the Dy catalyst as the most active and effective in this series, we subsequently examined the MMBL polymerization by this catalyst in more detail, specifically concerning the degree of control and kinetics of the polymerization. We chose DCM as the solvent because the polymerization in DMF is too rapid to be suitable for kinetic profiling by analyzing the reaction aliquots using NMR techniques (e.g., with a 0.25 mol % catalyst loading, the polymerization in DMF takes <1 min to achieve a quantitative monomer conversion).

Table 6 summarizes selected kinetic results of the MMBL polymerization with two different [MMBL]/[Dy] ratios at 25 °C in DCM (selected out of five different ratios ranging from 200 to 1600): a medium ratio of 400 (0.25 mol %

Table 5. Results of MMBL Polymerization by Dy Dialkyl at Varying Temperature[a]

run no.	temp (°C)	time (min)	conv. (%)	$10^4 M_n$ (g/mol)	MWD (M_w/M_n)	I^* (%)	[*rr*] (%)	[*mr*] (%)	[*mm*] (%)
33	25	1	100	3.69	1.64	122	36.3	55.6	8.1
34	0	240	100	5.95	1.82	76	30.4	57.5	12.1
35	−65	240	63.4	13.5	1.86	21	34.0	50.4	15.6

[a] Conditions: 3.0 mL of DMF, 4.08 mmol MMBL, 10.2 μmol Dy complex, [MMBL]/[Dy] 400/1.

Table 6. Selected Kinetic Data for MMBL Polymerization by Dy Dialkyl in DCM at 25 °C

run no.	[Dy] (mmol/L)	$[MMBL]_0/[Dy]_0$	time (min)	conv. (%)	$10^3 M_n$ (g/mol)	MWD (M_w/M_n)	I^* (%)
36	2.74	400	0.33	23.2	8.30	2.65	126
37			0.78	33.2	11.1	2.98	135
38			1.17	40.4	13.2	3.03	138
39			1.50	45.1	14.5	2.95	140
40			2	51.6	16.3	3.04	142
41			3	59.8	18.2	3.07	147
42			4	67.2	20.3	2.89	148
43			5	71.1	21.8	2.96	146
44			7	80.2	24.5	2.80	147
45			15	93.2	29.9	2.58	121
46			20	100	31.6	2.62	143
47	0.912	1200	1	8.2	16.6	5.32	67
48			3	12.8	29.1	4.20	60
49			6	26.8	39.6	3.55	91
50			10	36.2	54.3	2.92	90
51			15	45.3	62.4	2.75	98
52			20	51.3	69.8	2.60	99
53			30	62.0	84.2	2.34	99
54			40	77.8	95.9	2.18	109
55			90	96.3	107	1.90	121

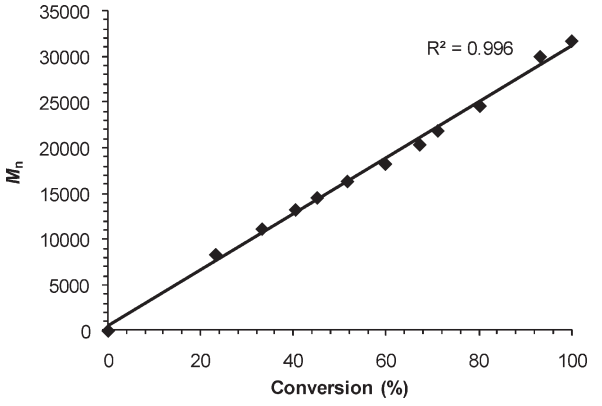

Figure 4. Plots of M_n versus MMBL conversion. Conditions: $[MMBL]_0/[Dy]_0$ = 400, DCM, 25 °C.

catalyst loading) and a high ratio of 1200 (0.083 mol % catalyst loading). As can be seen from this Table, the MMBL polymerization with a catalyst loading of 0.25 mol % is rapid, achieving a quantitative monomer conversion in 20 min. The I^* values were greater than unity (∼120−150%) at all conversions (runs 36−46), whereas the M_n of the resulting PMMBL increases linearly with the MMBL conversion (R^2 = 0.996, Figure 4). This ability of the catalyst to control the polymer MW was also reaffirmed in the polymerization with a lower catalyst loading of 0.083 mol % (runs 47−55), showing again a linear relationship between the polymer M_n and monomer conversion (R^2 = 0.974, Figure 5).

Kinetic experiments employed the $[MMBL]_0/[Dy]_0$ ratios ranging from 200 to 1600 (i.e., eight-fold catalyst concentration variations, while keeping the monomer concentration constant), showing a first-order dependence on [MMBL] for all ratios investigated (Figure 6). Furthermore, a double logarithm plot (Figure 7) of the apparent rate constants (k_{app}), obtained from the slopes of the best-fit lines to the

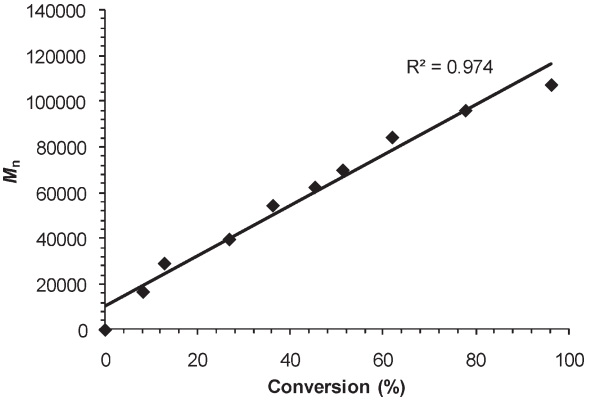

Figure 5. Plots of M_n versus MMBL conversion. Conditions: $[MMBL]_0/[Dy]_0$ = 1200, DCM, 25 °C.

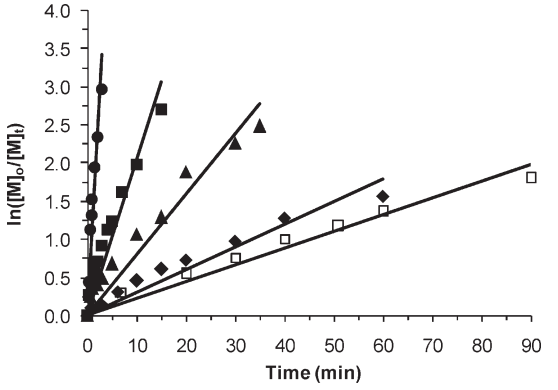

Figure 6. First-order plots of $Ln([M]_t/[M]_0)$ versus time for the MMBL polymerization by Dy in CH_2Cl_2 at 25 °C and varied catalyst concentrations: $[MMBL]_0$ = 1.09 M; $[Dy]_0$ = 5.47 (●), 2.74 (■), 1.37 (▲), 0.912 (◆), and 0.684 mM (□).

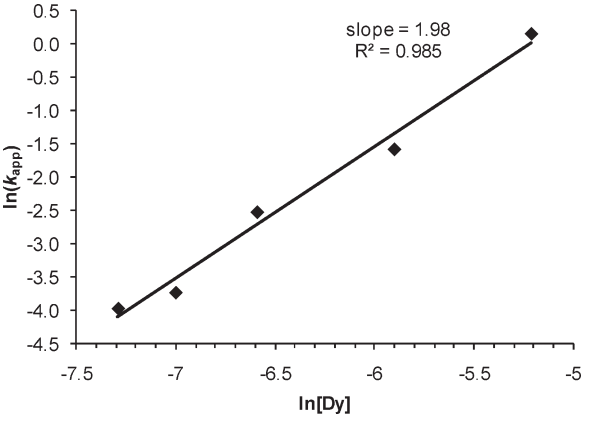

Figure 7. Plot of $\ln(k_{app})$ versus ln[Dy] for the MMBL polymerization by Dy in CH_2Cl_2 at 25 °C.

plots of $\ln([MMBL]_0/[MMBL]_t)$ versus time as a function of $\ln[Dy]_0$ was fit to a straight line (R^2 = 0.99) with a slope of 1.98. Therefore, the kinetic order with respect to [Dy], given by the slope of ∼2, reveals that the polymerization is second

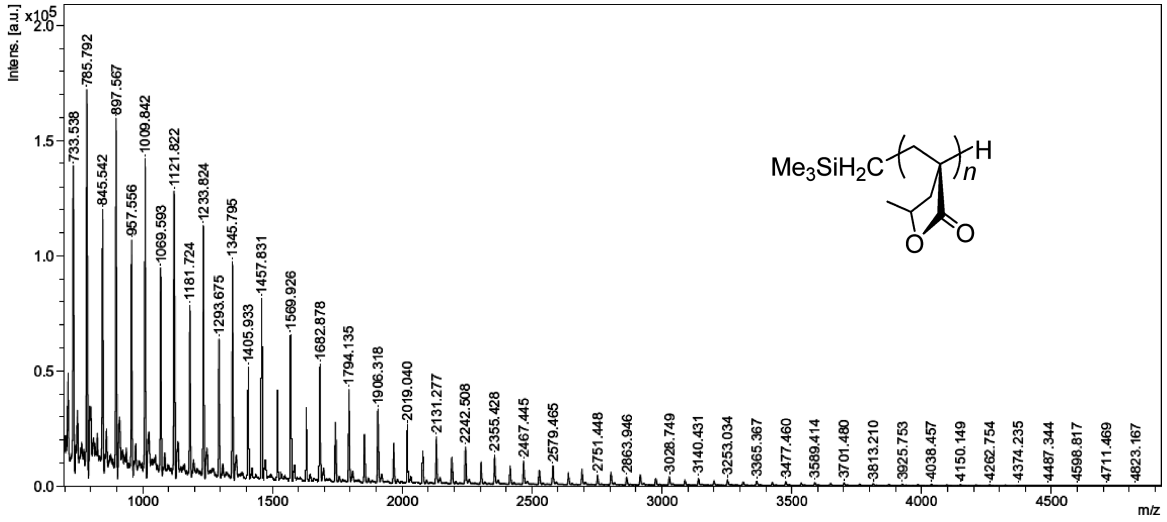

Figure 8. MALDI-TOF mass spectrum of the low-molecular-weight PMMBL produced by the Dy catalyst in DMF at 25 °C with $[MMBL]_0/[Dy]_0$ 20:1. The sample analyzed was quenched and unpurified, and the polymer chain-end structure corresponds to the major series of the peaks.

Scheme 2. Proposed Propagation "Catalysis" Cycle for MMBL Polymerization Catalyzed by the Dy Catalyst

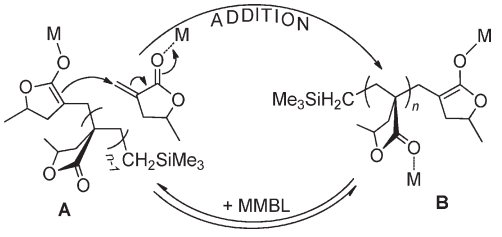

order in catalyst concentration; these kinetics results suggest a bimolecular propagation, analogous to the bimetallic mechanism established for the nonbridged group 4 metallocene catalysts,[39] for the MMBL polymerization by this half-sandwich complex, as proposed in Scheme 2. The propagation "catalysis" cycle in this mechanism involves Michael addition of REM-centered ester enolate propagating species **A** to the MMBL coordinated to (activated by) a second REM center, followed by the release of the coordinated REM catalyst to the ester oxygen of the polymer chain in **B** by the incoming monomer to regenerate the propagating species **A** and the activated monomer. If the release of the catalyst from the polymer chain to the incoming monomer was fast relative to the addition step and the equilibrium favored the formation of the activated monomer, then application of the steady-state approximation of the intermediate **B** would result in first-order kinetics with respect to the concentration of active species **A** and the activated monomer (i.e., second-order in [REM]) but zero-order kinetics in monomer concentration. However, the first-order dependence of monomer concentration we observed (Figure 6) implies that coordination of the REM catalyst to the ester group of the polymer chain and to the monomer is competitive. Hence, the concentration of the activated monomer now depends on monomer conversion, and there is a first-order dependence on monomer concentration, similar to what we previously observed in the MMA polymerization system by lithium ester enolates in combination with a bulky aluminum Lewis acid.[40] It seemed counterintuitive for such sterically open half-sandwich catalysts to adopt a bimetallic propagation pathway, but it made sense considering more than one growing chain per metal center and each chain end presumably also coordinated to the same metal serving as a

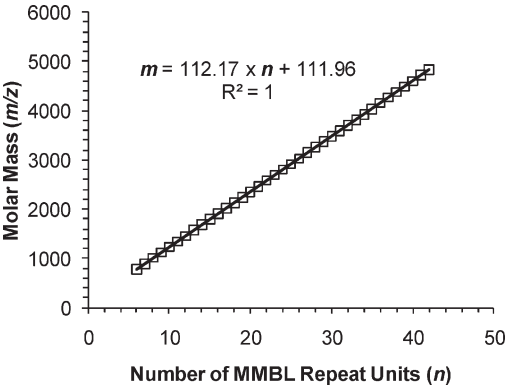

Figure 9. Plot of m/z values of the major series from Figure 8 versus the number of MMBL repeat units (n).

bulky chelating ligand. Propagation through oxygen-bridged dinuclear intermediates is also a possibility.

To identify the initiation and termination chain-end groups of the resulting PMMBL (therefore the chain initiation and termination pathways), a low-molecular-weight PMMBL sample produced by the Dy catalyst in a $[MMBL]_0/[Dy]_0$ ratio of 20:1 was analyzed by MALDI-TOF mass spectrometry (Figure 8). There are two series of mass distributions, both of which have mass differences between the peaks representing the molar mass of the MMBL repeat unit (112 g/mol). A plot of m/z values of the major series of peaks in the MALDI-TOF mass spectrum versus the number of MMBL repeat units (n) yielded a straight line with a slope of 112.2 and an intercept of 111.96 (Figure 9). The slope corresponds to the mass of the MMBL monomer, whereas the intercept is a sum of the masses of Na^+ (from the added NaI) and the chain-end groups, which correspond to a formula of $C_4H_{12}Si$. Hence, this analysis shows that the polymer has a structural formula of $Me_3SiCH_2-(MMBL)_n-H$, where the initiation chain end (Me_3SiCH_2-) was derived from the initiating trimethylsilylmethyl group within the Dy catalyst and the termination chain end (H) from the HCl-acidified methanol during the workup procedure. A plot of m/z values of the minor series of peaks in the MALDI-TOF mass spectrum versus the number of MMBL repeat units (n) yielded the same slope of 112.2 but a different intercept of 59.77 (or plus 112.2), the structure of which is currently unknown but presumably derived from chain transfer processes.

Table 7. Results of MMBL Polymerization by Dy Dialkyl in the Presence of CTA[a]

run no.	solvent	organo acid (CTA)	[MMBL]/[CTA]/[Dy]	time (min)	conv. (%)	$10^4 M_n$ (g/mol)	MWD (M_w/M_n)	I^* (%)
56	DMF	none	400/0/1	1	100	3.69	1.64	122
57	DMF	MBO	400/10/1	20	100	3.42	1.74	131
58	DMF	MBO	400/30/1	1440	77.0	2.57	1.96	135
59	DMF	MBO	400/50/1	1440	32.8	1.35	1.49	109
60	DCM	none	400/0/1	20	100	3.16	2.62	143
61	DCM	MBO	400/10/1	60	100	4.35	2.23	103
62	DCM	MBO	400/30/1	1440	93.1	3.09	3.85	135
63	DCM	MBO	400/50/1	1440	74.8	3.06	4.15	109
64	DMF	none	500/0/1	1	100	4.74	1.79	118
65	DMF	MIB	500/10/1	15	100	4.60	1.75	122
66	DMF	MIB	500/30/1	480	100	4.72	1.79	119
67	DMF	MIB	500/50/1	480	100	4.53	1.74	124

[a] Conditions: 3.0 mL of solvent, 4.08 mmol MMBL, 10.2 μmol Dy complex for a [MMBL]/[Dy] ratio of 400/1 or 8.16 μmol Dy complex for a [MMBL]/[Dy] ratio of 500/1, 25 °C; CTA: 3-methyl-2-butanone (MBO) or methyl isobutyrate (MIB).

One notable feature about the (M)MBL polymerization by these half-sandwich REM catalysts is the observed greater or much greater than 100% catalyst efficiencies for most of the polymerization runs (vide supra), suggesting that both alkyl groups on the metal participate in chain initiation. However, the observed first-order dependence on monomer implies that only one chain on the metal can grow at a time. The relatively broad MWDs observed for the polymers produced herein seem consistent with this scenario. Furthermore, the NMR-scale reaction of the Lu catalyst (the Dy catalyst is paramagnetic) with 10 equiv of MMBL at RT in CD_2Cl_2 showed the immediate formation of PMMBL and complete disappearance of the methylene resonances (−1.18 ppm, AB quartet) in Lu−CH_2SiMe$_3$ (which moved by ∼1.2 ppm to downfield now overlapping with other TMS resonances centered at ∼0 ppm), consistent with MMBL addition into both Lu−CH_2SiMe$_3$ bonds for the reaction carried out at RT. When the same reaction was monitored starting at −70 °C (no reaction) and gradually warming to −60 °C, the reaction went slowly, and the intensity of the CH_2SiMe$_3$ signal decreased as the polymer peaks started to grow. However, there was no further decrease in the CH_2SiMe$_3$ signal intensity after being reduced by 20.5%, although the monomer continued to be consumed and converted to polymer. These results imply that under this controlled polymerization condition at low temperatures, once initiated, the monomer is added preferentially to the Lu−enolate bond−derived from chain initiation involving nucleophilic attack of the alkyl ligand to the coordinated monomer[1] while leaving a large amount of the catalyst unconsumed. This scenario would then substantially inflate the polymer MW, thus giving rise to much lower catalyst efficiencies. This analysis is consistent with the polymerization results carried out at various temperatures (Table 5): when the polymerization temperature decreased from 25 to 0 and −65 °C, the catalyst efficiency decreased from 122 (run 33) to 76 (run 34) and 21% (run 35), respectively. Impressively, the catalyst efficiency of 21%, calculated based on the measure M_n (relative to the calculated M_n) of the polymer produced at −65 °C, matches well with the NMR result on the percentage of the catalyst participated in the polymerization at this temperature (20.5%).

Attempted Catalytic Polymerization of MMBL in the Presence of Organo Acids. To render catalytic production of polymer chains in the coordination−addition polymerization catalyzed by metal complexes, a suitable CTA added externally must effectively cleave the growing polymer chain from the active center, and the resulting new species containing part of the CTA moiety (typically in its deprotonated form) must efficiently reinitiate the polymerization.[1] It has been shown that organic acids such as alkyl thiols and enolizable ketones are effective CTAs to transform the living MMA polymerization by Cp*$_2$SmMe(THF) into a chain transfer polymerization for the catalytic production of PMMA, although the effectiveness for the catalytic polymer production by this system is still limited (turnover number, TON = 5), even with a [CTA]/[Sm] ratio as high as 29.[41] We previously showed that among the three organic acids investigated to promote the catalytic polymerization of MBL by Cp*$_2$Sm(THF)$_2$, MBO is most effective (TON = 10 with 20 equiv of MBO per metal), followed by MIB, whereas dimethyl malonate (DMM) completely halts the polymerization,[21] similar to the zirconocenium-catalyzed MMA polymerization in the presence of DMM.[42]

In light of these prior findings, we initially focused on MBO. It can be seen from Table 7 that the addition of MBO to the MMBL polymerization catalyzed by the Dy catalyst in a fixed [MMBL]/[Dy] ratio of 400/1 did not significantly alter the catalyst efficiency (I^* values) upon variations of equiv of MBO per metal from 0 to 10, 30, and 50 in DMF (runs 56−59) or in DCM (runs 60−64), except for the sharp drop in activity with an increase in equiv of MBO added to the system. Next, we switched to MIB, but it performed similarly to MBO. Specifically, the catalyst efficiency remained nearly constant (I^* = 118−124%, runs 64−67) for the MMBL polymerization in the presence of 0, 10, 30, or 50 equiv of MIB. Overall, these two organo acids investigated herein, which had been shown to be effective in promoting catalytic polymerization by the prototype sandwich REM catalyst, are ineffective for the half-sandwich Dy catalyst, attributable to either the inability of the two current CTAs to cleave the metal−polymer bond or the inefficient reinitiation of the species that resulted from such bond cleavage. These results further highlight the differences in catalytic behavior between sandwich and half-sandwich REM catalysts.

Conclusions

While being mediocre catalysts for polymerizations of MMA and MBL, all four half-sandwich REM dialkyl catalysts investigated herein are extremely active for polymerization of MMBL in DMF. Specifically, these catalysts can achieve a quantitative monomer conversion in DMF in <1 min with a catalyst loading of 0.20 mol %, giving a high TOF $> 30\,000$ h^{-1} for this catalyst system, which is at least 10 times higher than the sandwich REM catalyst Cp*$_2$Sm(THF)$_2$. The polymerization in DCM is slower, but all catalysts can achieve a quantitative monomer conversion in 20 (Y, Dy), 30 min (Lu), or 120 min (Sc). The activity trend of Dy ≥ Y > Lu > Sc is the same for both MBL and MMBL polymerizations: the largest Dy and Y metals are most active, whereas the smallest Sc catalyst is least active, with the Lu catalyst lying somewhere in the middle. The PMMBLs produced are syndio-rich atactic materials with high T_g values ranging from 217 (by Sc) to 222 °C (by Lu).

The ability of such half-sandwich REM dialkyl catalysts to control the resulting polymer MW has been demonstrated by the Dy catalyst, the most active and effective catalyst within this series, as evidenced by linear relationships between M_n of PMMBL and the [MMBL]/[Dy] ratio (from 200, 0.5 mol % catalyst, to 1600, 0.0625 mol % catalyst) and between M_n of PMMBL and monomer conversion at a give ratio. Hence, PMMBL with a medium M_n of 1.89×10^4 Da and MWD of 1.99 to a high M_n of 1.63×10^5 Da and MWD of 1.65 have been readily prepared. Kinetic experiments using the Dy catalyst have revealed a first-order dependence on [MMBL] but a second-order dependence on [Dy], indicating a bimolecular propagation involving two Dy metal centers in the rate-limiting C−C bond forming step (Scheme 2). Each metal center can carry more than one polymer chain and grow only one at a time, which originated from initiation with both alkyl groups on the metal and the first-order dependence on the monomer. The polymer chain end groups have been characterized by MALDI-TOF mass spectrometry, whereas the more-than-one-chain-per-metal scenario has been evidenced by the results of NMR studies and by typically greater or much greater than 100% catalyst efficiencies.

Enolizable organo acids, MBO and MIB, both of which are effective CTAs in promoting catalytic polymerization by the prototype sandwich REM catalysts, are ineffective for the half-sandwich Dy catalyst. These results further highlight the large differences in catalytic behavior between sandwich and half-sandwich REM catalysts.

Acknowledgment. The work carried out at CSU was supported by the U.S. National Science Foundation (NSF-1012326), whereas the work carried out at SIOC was supported by the National Natural Science Foundation of China (grant no. 20821002) and Shanghai Municipal Committee of Science and Technology (grant no. 07JC14063).

References and Notes

(1) Chen, E. Y.-X. *Chem. Rev.* **2009**, *109*, 5157–5214.
(2) (a) Yasuda, H. *Prog. Polym. Sci.* **2000**, *25*, 573–626. (b) Yasuda, H. *J. Polym. Sci., Part A: Polym. Chem.* **2001**, *39*, 1955–1959. (c) Nakayama, Y.; Yasuda, H. *J. Organomet. Chem.* **2004**, *689*, 4489–4498.
(3) Nishiura, M.; Hou, Z. *Nature Chem.* **2010**, *2*, 257–268.
(4) Tanaka, K.; Furo, M.; Ihara, E.; Yasuda, H. *J. Polym. Sci., Part A: Polym. Chem.* **2001**, *39*, 1382–1390.
(5) Okuda, J. *Dalton Trans.* **2003**, 2367–2378.
(6) Jian, Z.; Zhao, W.; Liu, X.; Chen, X.; Tang, T.; Cui, D. *Dalton Trans.* **2010**, *39*, 6871–6876.
(7) Kirillov, E.; Toupet, L.; Lehmann, C. W.; Razavi, A.; Carpentier, J.-F. *Organometallics* **2003**, *22*, 4467–4479.
(8) Zi, G.; Li, H.-W.; Xie, Z. *Organometallics* **2002**, *21*, 1136–1145.
(9) Yao, Y.; Zhang, Y.; Zhang, Z.; Shen, Q.; Yu, K. *Organometallics* **2003**, *22*, 2876–2882.
(10) Fabri, F.; Muterle, R. B.; de Oliveira, W.; Schuchardt, U. *Polymer* **2006**, *47*, 4544–4548.
(11) (a) Coates, G. W.; Hillmyer, M. A. *Macromolecules* **2009**, *42*, 7987–7989. (b) Gandini, A. *Macromolecules* **2008**, *41*, 9491–9504. (c) Tullo, A. H. *Chem. Eng. News* **2008**, *86*, 21–25. (d) Williams, C. K.; Hillmyer, M. A. *Polym. Rev.* **2008**, *48*, 1–10. (e) Meier, M. A. R.; Metzger, J. O.; Schubert, S. *Chem. Soc. Rev.* **2007**, *36*, 1788–1802.
(12) Mullin, R. *Chem. Eng. News* **2004**, *82*, 29–37.
(13) Hoffman, H. M. R.; Rabe, J. *Angew. Chem., Int. Ed. Engl.* **1985**, *24*, 94–110.
(14) (a) Manzer, L. E. *ACS Symp. Ser.* **2006**, *921*, 40–51. (b) Manzer, L. E. *Appl. Catal., A* **2004**, *272*, 249–256.
(15) Akkapeddi, M. K. *Polymer* **1979**, *20*, 1215–1216.
(16) Stansbury, J. W.; Antonucci, J. M. *Dent. Mater.* **1992**, *8*, 270–273.
(17) Akkapeddi, M. K. *Macromolecules* **1979**, *12*, 546–551.
(18) (a) Kimura, Y.; Nakamura, S. JP 046560 A, 2009. (b) Pickett, J. E.; Ye, Q.U.S. Patent 2007/0122625, 2007. (c) Bandenburg, C. J. WO 069926, 2004.
(19) (a) Mosnáček, J.; Yoon, J. A.; Juhari, A.; Koynov, K.; Matyjaszewski, K. *Polymer* **2009**, *50*, 2087–2094. (b) Mosnáček, J.; Matyjaszewski, K. *Macromolecules* **2008**, *41*, 5509–5511. (c) Ueda, M.; Takahashi, M.; Imai, Y.; Pittman, C. U., Jr. *J. Polym. Sci., Polym. Chem. Ed.* **1982**, *20*, 2819–2828. (d) Gridnev, A. A.; Ittel, S. D. WO 035960 A2, 2000.
(20) Sogah, D. Y.; Hertler, W. R.; Webster, O. W.; Cohen, G. M. *Macromolecules* **1987**, *20*, 1473–1488.
(21) Miyake, G. M.; Newton, S. E.; Mariott, W. R.; Chen, E. Y.-X. *Dalton Trans.* **2010**, *39*, 6710−6718 (appeared in the themed issue entitled "New Horizons in Organo-f-Element Chemistry").
(22) van den Brink, M.; Smulders, W.; van Herk, A. M.; German, A. L. *J. Polym. Sci., Polym. Chem. Ed.* **1999**, *37*, 3804–3816.
(23) Koinuma, H.; Sato, K.; Hirai, H. *Makromol. Chem., Rapid Commun.* **1982**, *3*, 311–315.
(24) Lee, C.; Hall, H. K. *Macromolecules* **1989**, *22*, 21–25.
(25) Trumbo, D. L. *Polym. Bull.* **1991**, *26*, 271–275.
(26) Cockburn, R. A.; McKenna, T. F. L.; Hutchinson, R. A. *Macromol. Chem. Phys.* **2010**, *211*, 501–509.
(27) Qi, G.; Nolan, M.; Schork, F. J.; Jones, C. W. *J. Polym. Sci., Polym. Chem. Ed.* **2008**, *46*, 5929–5944.
(28) Bandenburg, C. J. U.S. Patent 6,841,627 B2, 2005.
(29) Suenaga, J.; Sutherlin, D. M.; Stille, J. K. *Macromolecules* **1984**, *17*, 2913–2916.
(30) Miyake, G. M.; Zhang, Y.; Chen, E. Y.-X. *Macromolecules* **2010**, *43*, 4902–4908.
(31) Xu, X.; Chen, Y.; Sun, J. *Chem.—Eur. J.* **2009**, *15*, 846–850.
(32) Xu, X.; Chen, Y.; Feng, J.; Zou, G.; Sun, J. *Organometallics* **2010**, *29*, 549–553.
(33) Allen, R. D.; Long, T. E.; McGrath, J. E. *Polym. Bull.* **1986**, *15*, 127–134.
(34) (a) Bochmann, M.; Lancaster, S. J. *J. Organomet. Chem.* **1992**, *434*, C1–C5. (b) Chien, J. C. W.; Tsai, W.-M.; Rausch, M. D. *J. Am. Chem. Soc.* **1991**, *113*, 8570–8571.
(35) (a) Favarger, F.; Ginglinger, C. G.; Monchaud, D.; Lacour, J. *J. Org. Chem.* **2004**, *69*, 8521–8524. (b) Lee, H. S.; Novak, B. *Polym. Prepr.* **2005**, *46*, 839–840.
(36) (a) Rodriguez-Delgado, A.; Mariott, W. R.; Chen, E. Y.-X. *Macromolecules* **2004**, *37*, 3092–3100. (b) Bolig, A. D.; Chen, E. Y.-X. *J. Am. Chem. Soc.* **2004**, *126*, 4897–4906.
(37) (a) Yasuda, H.; Yamamoto, H.; Yamashita, M.; Yokota, K.; Nakamura, A.; Miyake, S.; Kai, Y.; Kanehisa, N. *Macromolecules* **1993**, *26*, 7134–7143. (b) Yasuda, H.; Yamamoto, H.; Yokota, K.; Miyake, S.; Nakamura, A. *J. Am. Chem. Soc.* **1992**, *114*, 4908–4909.
(38) Nguyen, H.; Jarvis, A. P.; Lesley, M. J. G.; Kelly, W. M.; Reddy, S. S.; Taylor, N. J.; Collins, S. *Macromolecules* **2000**, *33*, 1508–1510.
(39) (a) Stojcevic, G.; Kim, H.; Taylor, N. J.; Marder, T. B.; Collins, S. *Angew. Chem., Int. Ed.* **2004**, *43*, 5523–5526. (b) Li, Y.; Ward, D. G.; Reddy, S. S.; Collins, S. *Macromolecules* **1997**, *30*, 1875–1883.
(40) Rodriguez-Delgado, A.; Chen, E. Y.-X. *J. Am. Chem. Soc.* **2005**, *127*, 961–974.
(41) Nodono, M.; Tokimitsu, T.; Tone, S.; Makino, T.; Yanangase, A. *Macromol. Chem. Phys.* **2000**, *201*, 2282–2288.
(42) Mariott, W. R.; Rodriguez-Delgado, A.; Chen, E. Y.-X. *Macromolecules* **2006**, *39*, 1318–1327.